

Raman Scattering Study of Cation-Deficient $\text{Ba}_n(\text{MoNb})_{n-\delta}\text{O}_{3n-x}$ and Related Perovskite-like Oxides

A. A. Brown Holden and M. Reedyk*

Department of Physics, Brock University, St. Catharines, ON, L2S 3A1 Canada

E. García-González, M. Parras, and J. M. González-Calbet

Departamento Química Inorgánica, Facultad de Ciencias Químicas, Universidad Complutense de Madrid, 28040 Madrid, Spain

Received January 21, 2000. Revised Manuscript Received May 15, 2000

The Raman scattering spectra of $\text{Ba}_3\text{MoNbO}_{8.5}$ and $\text{Ba}_7\text{Nb}_4\text{MoO}_{20}$, two cation-deficient perovskite-like oxides, are presented for the first time and analyzed in an attempt to confirm the distribution of octahedra and tetrahedra proposed in recent structural investigations. The Raman spectra are discussed in relation to spectra of compounds of the hexagonal perovskite-like oxides with the general formula $\text{A}_n\text{B}_{n-\delta}\text{O}_{3n-x}$ ($\delta \geq 1$, $x \geq 0$). While the spectra of all compounds are found to be dominated by strong tetrahedral bands near 300 and 800 cm^{-1} , modes of octahedral symmetry are evident between 400 and 700 cm^{-1} in those compounds which contain octahedral $[\text{BO}_6]$ groups according to structural studies. The Raman spectrum of $\text{Ba}_3\text{Nb}_2\text{O}_8$ contains modes in the region attributed to vibrations of octahedral symmetry although it is stoichiometrically identical to the palmierite structure which has only tetrahedrally coordinated B-sites. This observation is in disagreement with structural work previously reported in the literature but provides strong corroborating evidence for a new study which indicates a variant stacking arrangement of hexagonal and cubic close-packed layers giving rise to an equal number of octahedrally and tetrahedrally coordinated B-sites in this compound.

Introduction

The perovskite structure, ABO_3 , where A is a large cation and B is a smaller, typically metallic cation, forms the basis of many interesting and extensively studied systems of compounds including the cuprate-based high- T_C superconductors and the more recently discovered manganese oxides exhibiting a colossal magnetoresistivity. The focus on, and effort expended in, investigating such systems is a consequence of the fact that the perovskite structure can accommodate an enormous number of different cations, and new compositions and structures with a wide range of magnetic, electronic, and optical properties can be formed by inserting buffer layers, varying stacking sequences, and introducing disorder via doping by chemical substitution or through vacancies. The variation in structures and their stoichiometry has been discussed by Katz and Ward¹ in terms of stacking of close-packed AO_3 layers. Stacking these layers in a close-packed arrangement leads to the formation for each AO_3 unit of an oxygen octahedron which is occupied by the B cation. Hexagonal (h) stacking of the layers occurs when the two neighboring layers are of the same type and results in octahedra which share faces, while cubic (c) stacking occurs when the neighboring layers are of different types and results in octahedra which share corners. When two octahedra share faces instead of corners, the B–B cation distance

decreases and the structure tends to be less stable. Often cationic vacancies are adopted on the B-sites in order to stabilize the structure, particularly in the case of B ions with large formal charge.

The system of perovskite-like compounds of the general formula $\text{A}_n\text{B}_{n-\delta}\text{O}_{3n-x}$ ($\delta \geq 1$, $x \geq 0$) are created by varying the ratio of cubic (c) and hexagonal (h) stacking of the $[\text{AO}_3]$ layers with B cations occupying octahedral cavities. When the cationic ratio of A to B is 3:2 ($n = 3$, $\delta = 1$), one of every three B sites remains unoccupied and different structures can be formed depending on composition and extent of anion-deficiency.² With $x = 0$ two polytypes can be adopted: the $\text{Cs}_3\text{Ti}_2\text{O}_9$ -type, where the AO_3 layers are hexagonal close packed and an empty octahedron is situated between face-sharing octahedra,³ and the 9R-type structure, where the stacking sequence is $(\text{hhc})_3$ and a vacant octahedral cavity is located between corner-sharing octahedra. The palmierite structure is derived from that of the 9R polytype when $x = 1$. In this case oxygen-deficient cubic AO_2 layers are formed which forces a change in coordination of the B atoms from octahedral to tetrahedral. The palmierite structure is shown schematically in Figure 1a.

(1) Katz, L.; Ward, R. *Inorg. Chem.* **1964**, *3*, 205.

(2) García-González, E.; Parras, M.; González-Calbet, J. M. *Chem. Mater.* **1998**, *10*, 1576.

(3) Mössner, B.; Kemmler-Sack, S. *J. Less-Common Met.* **1985**, *114*, 333.

* To whom correspondence should be addressed.

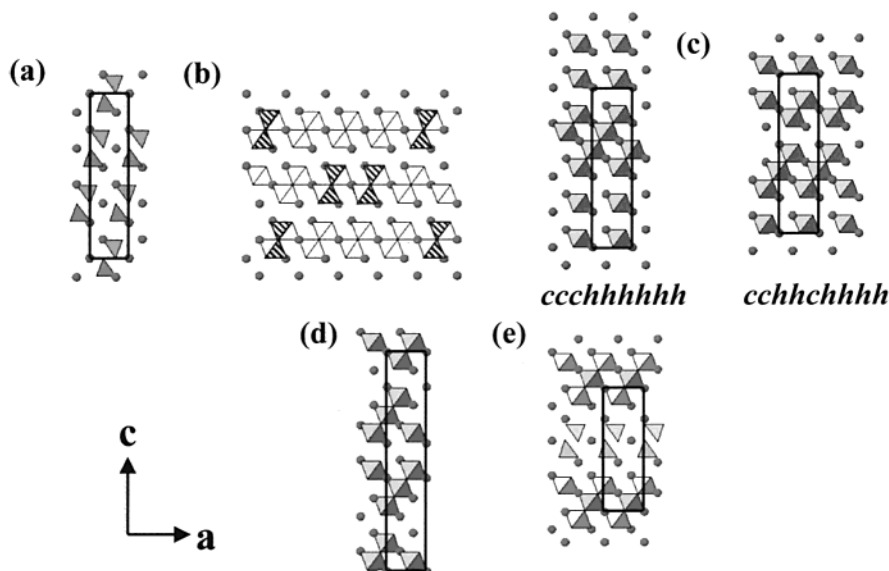


Figure 1. Schematic representation of the crystallographic structure of (a) palmierite $\text{Ba}_3\text{V}_2\text{O}_8$, (b) $\text{Ba}_3\text{MoNbO}_{8.5}$, (c) 9H $\text{Ba}_3\text{-Nb}_2\text{O}_8$ (two possible stacking arrangements shown), (d) 12R $\text{Ba}_3\text{LaNb}_3\text{O}_{12}$, and (e) 7H $\text{Ba}_7\text{MoNb}_4\text{O}_{20}$.

Barium and calcium orthovanadate, $\text{A}_3(\text{VO}_4)_2$, where $\text{A} = \text{Ba}$ and Ca , are members of this family of compounds of the palmierite-type structure and have been identified as possible materials for solid-state laser applications, where the optical center is formed by substitution of an ion such as Mn^{5+} at the tetrahedral lattice site.^{4–6} Calcium orthovanadate is furthermore a high-temperature ferroelectric with $T_C \approx 1100$ °C.⁷ Given the potential for applications it is of interest to further investigate the optical properties of these and related compounds in the $\text{A}_3\text{B}_2\text{O}_{9-x}$ family.

In addition to the A:B cationic ratio, the nature and the formal charge of the elements occupying the B framework determines the structural type adopted in these cationic deficient perovskites. Recently García-González and collaborators have investigated the crystal chemistry in the $\text{A}_n\text{B}_{n-6}\text{O}_{3n-x}$ system, with $\text{A} = \text{Ba}$ and mixed B-site occupancy of Nb and Mo, and have identified new cation-deficient perovskite-like ordered phases.^{2,8} $\text{Ba}_3\text{MoNbO}_{8.5}$ was found to have an oxygen stoichiometry between those of the 9R-polytype and the palmierite structure. Through electron diffraction and high-resolution electron microscopy they found that this new compound contains an ordered distribution of octahedra and tetrahedra in a 3:2 ratio in the cubic layers² as shown schematically in Figure 1b. For the $n = 7$ member, they found that a single phase compound was formed for the A:B = 7:5 ratio with Nb:Mo = 4:1.⁸ Their structural refinement showed that the 7H-polytype $\text{Ba}_7\text{MoNb}_4\text{O}_{20}$ is constituted of an ordered intergrowth along the c -axis of structural units corresponding to the 12R $\text{Ba}_4\text{B}_3\text{O}_{12}$ and $\text{Ba}_3\text{B}_2\text{O}_8$ palmierite polytypes. The structures of the 12R and 7H polytypes are shown schematically in Figure 1d,e, respectively.

Raman scattering is a useful optical technique for confirmation and identification of structural features and ordering in complex perovskite-based polytypes.^{9,10} The Raman scattering spectra of these new compounds in the Ba–Nb–Mo–O system are reported herein and interpreted in conjunction with information derived from the structural work.

To better understand the Raman scattering spectra of the Ba–Nb–Mo–O system we have also investigated several related compounds. The Raman-scattering spectrum of palmierite barium orthovanadate is well-known.^{3,11} We thus present the evolution of the Raman-scattering spectrum of palmierite $\text{Ba}_3\text{V}_2\text{O}_8$ as molybdenum and niobium are substituted into the vanadium sites. We find evidence for the presence of both octahedral and tetrahedral coordination in the new compound, $\text{Ba}_3\text{MoNbO}_{8.5}$, corroborating the results of the electron microscopy study of García-González and collaborators. We also find spectroscopic evidence for the fact that $\text{Ba}_3\text{-Nb}_2\text{O}_8$ does not have the simple palmierite structure as previously reported.⁹ The Raman scattering spectrum of the 7H compound $\text{Ba}_7\text{MoNb}_4\text{O}_{20}$ which can be described as an ordered intergrowth of blocks constituting 9R and 12R structures is compared to spectra of pure compounds of the 9R and 12R polytypes.

Experimental Section

Polycrystalline samples of $\text{Ba}_3\text{V}_2\text{O}_8$, $\text{Ba}_3\text{Nb}_2\text{O}_8$, $\text{Ba}_3\text{MoVO}_{8.5}$, Ba_3NbVO_8 , $\text{Ba}_3\text{NbMoO}_{8.5}$, $\text{LaBa}_3\text{Nb}_3\text{O}_{12}$, and $\text{Ba}_7\text{Nb}_4\text{MoO}_{20}$ were prepared from stoichiometric amounts of BaCO_3 (Aldrich, 99.98%), Nb_2O_5 (Aldrich, 99.5%), MoO_3 (Aldrich, 99.5%), La_2O_3 (Aldrich 99.99%), and V_2O_5 (Aldrich, 99.5%). After grinding, the powder was pressed into a pellet and subjected to a heating treatment dependent on the chemical composition as summarized in Table 1. The homogeneous product obtained in every case was slowly cooled to room temperature in the

(4) Brixner, L. H.; Flournoy, P. A. *J. Electrochem. Soc.* **1965**, *112*, 303.

(5) Whitmore, M. H.; Verdún, H. R.; Singel, D. J. *Phys. Rev. B* **1993**, *47*, 11479.

(6) Buijse, B.; Schmidt, J.; Chan, I. Y.; Singel, D. J. *Phys. Rev. B* **1995**, *51*, 6215.

(7) Glass, A. M.; Abrahams, S. C.; Ballmann, A. A.; Loiacono, G. *Ferroelectrics* **1978**, *17*, 579.

(8) García-González, E.; Parras, M.; González-Calbet, J. M. *Chem. Mater.* **1999**, *11*, 433.

(9) Kemmler-Sack, S.; Treiber, V.; Fadini, A. *Z. Anorg. Allg. Chem.* **1979**, *453*, 157.

(10) Setter, N.; Laulicht, I. *Appl. Spectrosc.* **1987**, *41*, 526.

(11) Grzechnik, A.; McMillan, P. F. *Solid State Commun.* **1997**, *102*, 569.

Table 1. Synthesis Conditions and Unit Cell Parameters Indexed on a Hexagonal Lattice with $\alpha = \beta = 90^\circ$, $\gamma = 120^\circ$ of $A_nB_{n-\delta}O_{3n-x}$ Compounds

	T ($^\circ\text{C}$)	t (days)	a (\AA)	c (\AA)
$Ba_3V_2O_8$	1100	4	5.7702	21.261
Ba_3VNbO_8	1200	5	5.8967	21.218
$Ba_3Nb_2O_8$	1250	4	5.901	20.909
$Ba_3VMo_{0.5}$	1100	7	5.835	21.34
$Ba_3NbMo_{0.5}$	1100	7	5.931	21.01
$LaBa_3Nb_3O_{12}$	1200	12	5.751	28.110
$Ba_7MoNb_4O_{20}$	1300	3	5.8644	16.5272

platinum crucibles used for the synthesis. Unit cell parameters were determined by X-ray powder diffraction on a Philips X'Pert diffractometer equipped with a bent copper monochromator and using Cu $K\alpha$ radiation.

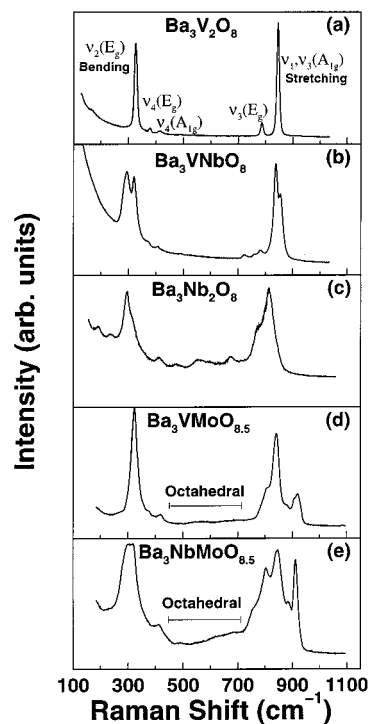
Unpolarized Raman spectra were measured at room temperature in a 90° scattering geometry using the 632.8 nm line of a helium–neon laser and a single-grating spectrograph (1200 grooves/mm) with thermoelectrically cooled CCD signal detection. A holographic notch filter was used to reject Rayleigh scattered light.

Results and Discussion

The X-ray diffraction patterns obtained for all of the compositions prepared indicated that the samples were single phase. The patterns for $Ba_3V_2O_8$, Ba_3VNbO_8 , and $Ba_3VMo_{0.5}$ resembled that of $Ba_3NbMo_{0.5}$ for which a detailed crystallographic analysis is presented in ref 2, and thus all were assigned on the basis of a 9R-type unit cell. The results for $Ba_3Nb_2O_8$ were surprisingly different from those previously reported in the literature,⁹ and it was assigned to a hexagonal lattice with a nine-layer sequence as discussed in ref 12. The pattern corresponding to $Ba_7Nb_4Mo_{20}$ was indexed on a 7H-type unit cell as previously reported.⁸ $Ba_3LaNb_3O_{12}$ was indexed on a rhombohedral 12R unit cell from data given in ref 13. The unit cell parameters are given in Table 1.

The Raman scattering spectra of the five $n = 3$ compositions investigated are given in Figure 2. All spectra have been corrected for the Bose temperature factor. The spectrum obtained for $Ba_3V_2O_8$ is in good agreement with previous work,^{3,11} as is the spectrum for $Ba_3VMo_{0.5}$.³

The palmierite structure adopted by $Ba_3V_2O_8$ has space group trigonal $D_{3d}^5\bar{R}3m$.¹⁴ A group theoretical analysis was carried out by following the procedure outlined by Rousseau, Bauman, and Porto¹⁵ with the crystallographic positions given by Durif¹⁴ and found to be in complete agreement with several already reported in the literature.^{3,11,16,17} The normal modes predicted by the group theoretical symmetry analysis are given in Table 2. The $A_{2u} + E_u$ are acoustic modes, the A_{1g} and E_g modes are Raman active, and the A_{2u} and E_u modes are infrared active. Of the Raman-active modes, $2A_{1g} + 3E_g$ are external modes due to translational vibrations of the Ba^{2+} cations and translational

**Figure 2.** Raman scattering spectra of (a) $Ba_3V_2O_8$, (b) Ba_3VNbO_8 , (c) $Ba_3Nb_2O_8$, (d) $Ba_3VMo_{0.5}$, and (e) $Ba_3NbMo_{0.5}$ at room temperature.**Table 2. Results of a Group Theoretical Symmetry Analysis for Various $A_nB_{n-\delta}O_{3n-x}$ Compounds**

	space group	normal modes
$Ba_3B_2O_8$	$D_{3d}^5\bar{R}3m$	$5A_{1g} + A_{1u} + A_{2g} + 6A_{2u} + 6E_g + 7E_u$
$Ba_4B_3O_{12}$	$D_{3d}^5\bar{R}3m$	$7A_{1g} + 2A_{1u} + 2A_{2g} + 8A_{2u} + 9E_g + 10E_u$
$Ba_7B_5O_{20}$	$D_{3d}^5\bar{P}3m1$	$12A_{1g} + 3A_{1u} + 3A_{2g} + 14A_{2u} + 15E_g + 17E_u$

and rotational oscillations of the $[VO_4]^{3-}$ tetrahedra. Raman bands below 200 cm^{-1} (not shown in Figure 2) have been attributed to these external modes.¹¹ The internal bending and stretching modes of the $[VO_4]^{3-}$ tetrahedra are $3A_{1g} + 3E_g + 3A_{2u} + 3E_u$. The internal modes of free $[VO_4]^{3-}$ ions of T_d symmetry are classified as ν_1 (symmetric stretching mode of A_1 symmetry), ν_2 (bending mode of E symmetry), ν_3 (antisymmetric stretching mode of F_2 symmetry), and ν_4 (bending mode of F_2 symmetry). It is customary to adopt this notation as well for the distorted tetrahedra in a crystalline environment such as that of $Ba_3V_2O_8$; however, the reduction of symmetry to C_{3v} results in internal ν_1 , ν_2 , ν_3 , and ν_4 modes with $A_{1g} + A_{2u}$, $E_g + E_u$, $A_{1g} + E_g + A_{2u} + E_u$, and $A_{1g} + E_g + A_{2u} + E_u$ symmetry, respectively.^{11,16} The assignment of the internal Raman bands for $Ba_3V_2O_8$ and their symmetry type is given, according to Grzechnik and McMillan,¹¹ in Figure 2a. Note that the highest frequency ν_1 and ν_3 modes of A_{1g} symmetry are not resolved as also observed in previous work.^{3,11} Grzechnik and McMillan showed that upon application of high pressure this band near 850 cm^{-1} splits due to an induced increase of distortion of the tetrahedral groups, thereby revealing the two modes. They assigned the higher frequency of the two to the ν_3 mode and the lower frequency one to the ν_1 mode.¹¹

Figure 2b shows the effect of 50% substitution of vanadium with niobium. The most notable change in the Raman spectrum is that the most intense bands

(12) García-González, E.; Parras, M.; González-Calbet, J. M., to be published.

(13) Von Rother, H. J.; Kemmler-Sack, S.; Treiber, U.; Cyris, W. *Z. Anorg. Allg. Chem.* **1980**, *466*, 131.

(14) Durif, A. *Acta Crystallogr.* **1959**, *12*, 420.

(15) Rousseau, D. L.; Bauman, R. P.; Porto, S. P. S. *J. Raman Spectrosc.* **1981**, *10*, 253.

(16) Grzechnik, A. *Chem. Mater.* **1998**, *10*, 1034.

(17) Kouk, M. H.; Lee, S. C.; Tang, S. H.; Ishibashi, Y. *Solid State Commun.* **1989**, *10*, 797.

split into two modes. The splitting is most likely due to the presence of two types of tetrahedra—those containing V and those containing Nb. In the band near 320 cm^{-1} , the higher component has the same frequency as the mode in $\text{Ba}_3\text{V}_2\text{O}_8$, suggesting that the lower component is due to bending motion in tetrahedra containing Nb.

Figure 2d shows the effect of substituting V by 50% Mo rather than Nb. The 320 cm^{-1} tetrahedral bending mode is noticeably broadened compared to the $\text{Ba}_3\text{V}_2\text{O}_8$ spectrum which may imply a small unresolved splitting. As typically found for other tetrahedrally coordinated oxides,¹⁸ the tetrahedral $[\text{MoO}_4]^{2-}$ ν_1 , ν_3 mode has a noticeably higher frequency than the equivalent $[\text{VO}_4]^{3-}$ mode yielding a large splitting of the high-frequency stretching mode. More notably, new bands are observed in the region between 450 and 700 cm^{-1} . The spectrum of $\text{Ba}_3\text{NbMoO}_{8.5}$ shown in Figure 2e is very similar. In this case a small splitting in the ν_2 bending mode seems to be just resolved. We interpret these additional features as internal modes of octahedrally coordinated Nb, Mo, or V cations whose presence is expected from the structural work of García-Gonzalez and collaborators.² This conclusion is drawn through comparison with typical frequencies reported in the literature for the modes of octahedrally coordinated $[\text{BO}_6]$ groups,^{18,19} and with the high pressure work of Grzechnik and MacMillan on $\text{Ba}_3\text{V}_2\text{O}_8$ who found that near 120 and 150 kbar there were pressure-induced phase transitions associated with structural rearrangement which, as a consequence, produced two additional much broader bands, centered near 770 and 620 cm^{-1} , respectively. These new bands were interpreted to arise as a result of a change in the coordination of the V cation from tetrahedral to octahedral.¹¹

The spectrum of $\text{Ba}_3\text{Nb}_2\text{O}_8$ shown in Figure 2c is curious because, in addition to strong bands near 300 and 800 cm^{-1} , several modes appear in the region between 450 and 700 cm^{-1} which we take as evidence for some octahedrally coordinated Nb sites; yet the oxygen stoichiometry has been found to be 8.¹² This implies that the sample of $\text{Ba}_3\text{Nb}_2\text{O}_8$ investigated here does not have the simple palmierite structure as previously reported⁹ but rather a more complicated stacking arrangement of polyhedra. Both electron and X-ray diffraction measurements as well as high-resolution electron microscopy were carried out in an effort to elucidate the structure of $\text{Ba}_3\text{Nb}_2\text{O}_8$.¹² It was found that the symmetry is hexagonal rather than rhombohedral as it is for the other $n = 3$ compounds investigated. From the structural study it was concluded that the 9H cell is formed by stacking six hexagonal (h) and three cubic (c) layers. The stacking sequence can be interpreted on the basis of two possibilities, (ccchhhhh) and (cchhchhh), which are shown in Figure 1c. From the topological point of view, both unit cells differ only in whether there is a cubic layer "breaking up" the block of hexagonal layers. The exact sequence is then difficult to determine incontrovertibly. In any case, the existence of five or seven face-sharing octahedra is stabilized

through the introduction of vacancies on the Nb sites. Ideally vacant and occupied octahedra would alternate along the stacking direction. However, from the uncertainty in the exact structure and from the relatively long period of the hexagonal block, it is more likely that the vacancies are disordered and hence there is effectively a fractional occupation of every cationic site in the block. The location of the anionic vacancies in any of the two possible sequences leads invariably to an equal number of octahedrally and tetrahedrally coordinated B-sites, like the $n = 3$ compounds with an $\text{O}_{8.5}$ anionic composition. This is because there are more face-shared octahedra than in the palmierite structure where the introduction of an oxygen deficient cubic layer in the ordered (hhc)₃ sequence results in only tetrahedra. Thus in agreement with our Raman scattering results, the presence of both octahedrally and tetrahedrally coordinated Nb is expected for $\text{Ba}_3\text{Nb}_2\text{O}_8$ even though the anionic composition is the same as that of the palmierite compounds which contain only tetrahedra.

Through comparison of the five spectra of Figure 2 we thus conclude that the pure palmierite-type spectrum containing only tetrahedra in the 9R structure occurs only with V or V/Nb. When Mo is introduced, and therefore the oxygen content increases, octahedral modes appear. If only Nb is present, tetrahedral as well as octahedral modes are observed, probably due to the fact that Nb(V) ions seldom occur in tetrahedral coordination in contrast to V(V) which is preferentially placed in tetrahedral sites.

As described in the Introduction, the 7H-polytype $\text{Ba}_7\text{Nb}_4\text{MoO}_{20}$ is constituted of a perovskite block of the palmierite composition $\text{Ba}_3\text{B}_2\text{O}_8$ alternating with a block of the 12R-polytype $\text{Ba}_4\text{B}_3\text{O}_{12}$. These three polytypes belong to the D_{3d} crystallographic point group. The normal modes predicted by a group theoretical symmetry analysis, carried out using the procedure outlined in ref 15, are compared in Table 2. The crystallographic positions of the atoms are given in ref 13 for the 12R-polytype and in ref 8 for the 7H-polytype. The A_{1g} and E_g modes are Raman active. Since the B-atoms are located at sites of C_{3v} symmetry in the three polytypes (as well as in the case of the 9R and 7H polytypes, at sites of D_{3d} symmetry which do not contribute Raman-active modes), one would expect to find very similar Raman spectra which is confirmed by the spectra shown in Figure 3a–c. Each spectrum is dominated by a band near 300 cm^{-1} and a set of bands near 800 cm^{-1} which we assign through comparison with the spectra for the $n = 3$ compounds to tetrahedral vibrations. Note, as was the case for $\text{Ba}_3\text{VMoO}_{8.5}$ and $\text{Ba}_3\text{NbMoO}_{8.5}$, that the Mo-containing 7H compound exhibits a tetrahedral $[\text{MoO}_4]^{2-}$ mode beyond 900 cm^{-1} . The weak features found between 500 and 700 cm^{-1} for the 12R and 7H compounds are assigned to modes arising from octahedrally coordinated B-sites which are expected for the 12R structure which consists of blocks of three face-sharing octahedra with a central void which are linked together through single corner-sharing octahedra.¹³

In summary, we have shown that the Raman scattering spectra of all of the $A_n\text{B}_{n-\delta}\text{O}_{3n-x}$ compounds investigated are dominated by two strong bands near 300 and 800 cm^{-1} which correspond to $[\text{BO}_4]$ tetrahedral groups (B = V, Nb, Mo). There are however subtle

(18) Nakamoto, K. *Infrared and Raman Spectra of Inorganic and Coordination Compounds, Part A: Theory and Applications in Inorganic Chemistry*, 5th ed.; Wiley: New York, 1997.

(19) Poeppelmeier, K. R.; Jacobson, A. J.; Longo, J. M. *Mater. Res. Bull.* **1980**, *15*, 339.

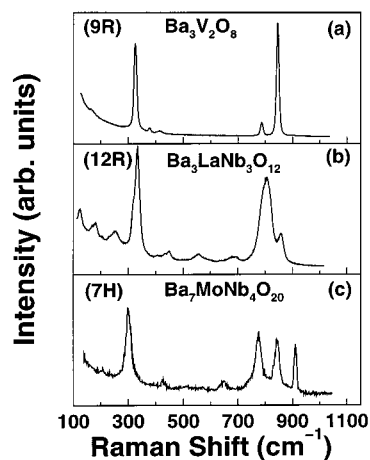


Figure 3. Raman scattering spectra of (a) 9R $Ba_3V_2O_8$, (b) 12R $Ba_3LaNb_3O_{12}$, and (c) 7H $Ba_7MoNb_4O_{20}$ at room temperature.

differences in the spectra which can be interpreted as due to unique structural features of the individual compounds. Most notably, the introduction of face-sharing octahedra in the palmierite structure leads to a meaningful change in the Raman spectrum. Modes attributed to octahedrally coordinated $[BO_6]$ groups are evident between 400 and 700 cm^{-1} in several compounds including $Ba_3NbMoO_{8.5}$, providing corroborating evi-

dence for previous structural work on this compound indicating an ordered arrangement of octahedra and tetrahedra. Of particular interest is $Ba_3Nb_2O_8$ which has an oxygen stoichiometry that is the same as that of the palmierite structure and yet has a Raman scattering spectrum that bears more similarity to the compounds with $O_{8.5}$ oxygen stoichiometry containing octahedra. This observation is however fully consistent with recent structural work showing that $Ba_3Nb_2O_8$ adopts a variant structure in which an equal number of octahedrally and tetrahedrally coordinated B sites exist. The presence of modes of octahedral symmetry was also apparent in the spectrum of $Ba_7Nb_4MoO_{20}$ as expected according to structural work indicating an ordered intergrowth of face-sharing octahedra and palmierite structural blocks in this compound. It is thus clear that the Raman scattering spectrum can provide valuable insight regarding structural differences in closely related and even stoichiometrically identical compounds.

Acknowledgment. Financial support was provided by the Natural Sciences and Engineering Research Council (NSERC) of Canada and by the CICYT (Spain) through Research Projects MAT95-0642 and MAT98-0648.

CM000037I